Hindawi
Mathematical Problems in Engineering
Volume 2023, Article ID 6776734, 11 pages
https://doi.org/10.1155/2023/6776734

Research Article

Research on Development Mechanism and Criterion of Upward Fractures in Longwall Face Mining

Jian Cao, Haitao Su, Jianwei Li, Xiangye Wu, and Eryu Wang

Institute of Mining Engineering and Coal, Inner Mongolia University of Science and Technology, Baotou, Inner Mongolia 014010, China

Correspondence should be addressed to Jian Cao; 2020913@imust.edu.cn

Received 21 September 2022; Revised 15 October 2022; Accepted 24 November 2022; Published 17 April 2023

Academic Editor: Fuqiang Ren

After mining, upward fractures develop from bottom to top, and they are key channel for groundwater and gas flow and also sand burst; therefore, it is important to study the development mechanism and criterion of upward fractures. Combining with physical simulation and theoretical analysis, the development law of mining-induced upward fractures was revealed, and the mechanism and criterion of fracture propagation was studied. The results show that the development of mining-induced upward fractures can be divided into the following three stages: with the face advances from the open cut, the vertical fractures are generated at the mining boundary, and the roof is flexural but not caved; it is "Fractures generate stage." After roof caves, the upward fractures extend and develop upward along the caving angle with continue advances; it is "Fractures develop and extend stage." When the face reaches critical mining, the development height of the upward fractures is at its maximum and is basically invariable; it is "Fractures stabilization stage." Mining-induced fractures can be analyzed as mixed-type fractures in fracture mechanics; when the combined stress exceeds the critical strength of stratum, it will extend downward until penetrate through the stratum, and the upward fracture develops and extends upwards. The parameter controlling the fracture of the rock stratum is the maximum hoop tensile stress $\sigma_{(\theta)\max}$, at the fracture end, the theoretical model of fracture propagation was established, and the criterion of upward fractures was proposed.

1. Introduction

The upward fractures are the key channel of water and gas conduction. In order to realize water conservation mining and mine disaster prevention, it is important to study the criterion of upward fractures. The development essence of upward fracture is that the concentrated stress reaches the tensile strength, it develops continuously with the face advances, and it finally reaches a stable stage.

Lots of research studies relating to the development law of upward fractures by field measurement have been published. Zhu and Teng [1] concluded that the development height of the upward fracture is directly proportional to the total mining thickness. Zhang and Zhang [2] analyzed the overburden of thick coal seam mining fracture propagation mechanics and principle based on the related theories of elastic-plastic and fracture mechanics. Bai and Tu [3] summarized the mining-induced fracture characteristics in shallow coal seam. Through engineering tests, Tan et al. [4] obtained the height of water-conducting fracturing zone. Huang et al. [5] studied the height of upward fracture by transient electromagnetic and drilling in Wanli mining area.

Besides, physical simulation, numerical calculation, and theoretical model were applied to study the development law of upward fractures. Wen et al. [6] established a fracture expansion model. By using the elasticity and Winkler foundation theory, Li et al. [7] established the numerical calculation model of fracture and the evolution of overburden strata under the condition of seepage-stress coupling and analyzed the dynamic change process of overburden strata fracture development height. By using physical simulation experiment, Bai et al. [8] revealed the failure mechanism of water-conducting fracture zone. Xu et al. [9, 10] revealed that the position of main key strata of

overlying strata will affect the upward crack development height of coal seam roof. Based on partial filling mining in shallow coal seams, Zhang and Huang [11] found that different backfilling parameters directly affect the development height of upward fractures. Zhao et al. [12] established the development height of upward fractures with the subsidence of key strata and analyzed the dynamic development process of upward fractures with the longwall face advances. Cao and Huang [13] obtained the development characteristics of fractures in shallow single seam mining and repeated mining, and the relationship between pillar staggered distance and fractures is revealed. Besides, fractal theory was used to quantitatively study the development process of fractures [14–28].

Above all, at present, based on various research methods, there are lots of studies on the upward fractures development in single seam and multiseams mining. Fractures development is a macroscopic phenomenon, which contains fracture generation and expansion fracture mechanics is an effective method to analyze the development of upward fracture; however, there are few studies in this area. Therefore, based on fracture propagation theory in fracture mechanics and physical simulation, the development law of mining-induced upward fractures was revealed in this paper, and mechanism and criterion of fracture propagation were studied.

2. Development Law of Mining-Induced Upward Fractures

2.1. Fractures Development Based on Physical Simulation Experiment

2.1.1. Fractures Development of No. 1-2 Coal Seam Mining in Daliuta Coal Mine

(1) Physical Simulation Experiment Model. Physical simulation experiment was established to reveal the development stage of mining-induced upward fractures. Based on the mining condition of the No. 1-2 coal seam in Daliuta Coal Mine, the average thickness of the coal seam is 4 m, and its buried depth is about 73 m. The experiment model is 1.5 m long × 1.3 m wide × 0.16 m height (Figure 1). Sand was adopted as the aggregates, cementitious materials are gypsum and calcium carbonate, and the material ratio is shown in Table 1.

(2) Fractures Development with Longwall Face Advances. The coal seam was excavated from left to right. When the longwall face advances to 15 m, the immediate roof caves. There is no fracture development in the overburden, and the roof caving height is 1.4 m, as shown in Figure 2.

When it advances to 46 m, the overlying strata above immediate roof suddenly cave, and it is the first caving of main roof. The roof caving angle is about 55°, as shown in Figure 3.

When it advances to 54 m, the main roof produces the first periodic caving, the development height of fracture reaches 20.5 m, the separation height of fracture is 3.2 m, and its separation width is 31.8 m. As the longwall face advances,

Figure 1: Physical simulation experiment model of Daliuta Coal Mine.

when the longwall face advances to 64 m, 76 m, . . ., 120 m, the main roof produces the 2nd, 3rd, . . ., 7th periodic roof caving, respectively, and simultaneously, the fractures develop upwards, as shown in Figure 4. When it advances to 120 m, it reaches critical mining, and the mining-induced fractures have developed to the ground surface (Figure 4(d)). The relationship between fracture development height and face advances distance is shown in Figure 5.

(3) The Relationship between Fractal Dimension and Face Advances Distance. The two-dimensional slice image is obtained from 3DEC numerical calculation, the image obtained is often RGB color image, and it is converted into gray image, the processed gray image is imported into MATLAB, and the image is binarized by using the threshold segmentation method. The gray transformation discriminant function of binary processing is as follows:

$$f(x, y) = \begin{cases} 0, & f(x, y) \le t, \\ 1, & f(x, y) \ge t. \end{cases} \quad (1)$$

FracLab toolbox is used to calculate the fractal dimension of the processed digital image, and the fractal dimensions of fractures with different advance distances are shown in Figure 6.

Figure 6 shows that in normal mining stage, the fractal dimension increases gradually while the longwall face advances, and when it reaches critical mining, the development height of fractures does not change significantly while the longwall face advances.

2.1.2. Fractures Development of No. 4-2 Coal Seam Mining in Hongliulin Coal Mine

(1) Physical Simulation Experiment Model. Taking the No. 4-2 coal seam mining in Hongliulin Coal Mine as the background, the average thickness of the coal seam is 2.1 m, and its buried depth is about 115.7 m. The experiment model is 2.0 m long × 1.5 m wide × 0.2 m height (Figure 7), the geometric similarity ratio is 1 : 200, and the material ratio is shown in Table 2.

(2) Fractures Development with Longwall Face Advances. The coal seam was excavated from left to right. When it advances to 22 m, the immediate roof caves and roof of longwall face is deflected, as shown in Figure 8. When it advances to 50 m,

Table 1: The material ratio of physical simulation experiment.

Lithology	Thickness (m)	Depth (m)	Consumables (kg)			
			Sand	Plaster	Calcium carbonate	Fly ash
Loess	21.79	21.79	Sand (37.69): loess (37.69): silicone oil (8.29)			
Fine-grained sandstone	6.03	27.82	19.21	0.73	1.81	
Siltstone	16.86	44.68	58.23	1.91	4.60	
Fine-grained sandstone	1.77	46.45	6.04	0.23	0.53	
Siltstone	1.50	47.95	5.18	0.17	0.41	
Fine-grained sandstone	0.95	48.90	3.24	0.12	0.28	
Medium-grained sandstone	4.13	53.03	14.09	0.37	1.40	
Coarse-grained sandstone	4.37	57.4	14.91	0.39	1.49	
Siltstone	2.54	59.94	8.77	0.30	0.68	
Fine-grained sandstone	3.86	63.80	13.18	0.48	1.15	
Siltstone	1.81	65.61	6.25	0.21	0.49	
Fine-grained sandstone	1.79	67.40	6.11	0.23	0.53	
Siltstone	2.33	69.73	8.05	0.27	0.62	
Fine-grained sandstone	1.87	71.60	6.38	0.24	0.56	
Medium-grained sandstone	1.36	72.96	4.64	0.12	0.46	
No. 1-2 coal seam	4.00	76.96	5.44	0.28	1.36	5.44
Siltstone	6.04	83.00	20.84	0.72	1.63	

Figure 2: The immediate roof caves.

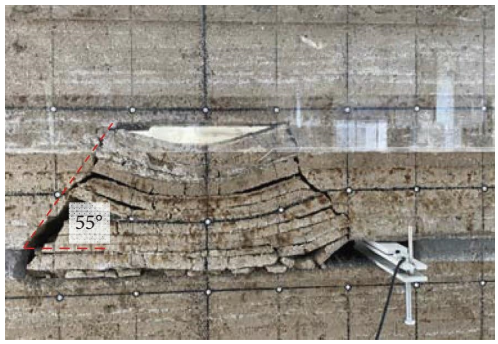

Figure 3: The first caving of main roof.

the overlying strata above the immediate roof suddenly cave, and it is the first caving of main roof; the roof caving angle is about 60°, as shown in Figure 9. When it advances to 50 m, the roof caving and fracture development are shown in Figure 10; when the longwall face reaches critical mining, the roof caving and fracture development are shown in Figure 11. It can be known that the fracture development height increases when the longwall face advances.

2.2. Development Stage of Mining-Induced Upward Fractures. With the longwall face advance, under the force of the concentrated tensile stress and gravity, the overlying strata gradually become flexural and then cave. At the same time, the upward fractures continue to develop upward along a certain caving angle, which is usually about 60. According to the development characteristics, the development of mining-induced upward fractures can be divided into the following three stages, and it is shown in Figure 12.

(1) Fractures generate stage: With the longwall face advances from the open cut, the vertical fractures are generated at the mining boundary, and the roof is flexural but not caved, as shown in Figure 12(a).

(2) Fractures develop and extend stage: After the roof caves, the upward fracture develops upward along the caving angle of the roof. With the longwall face advances and the roof caves from bottom to top, the upward fracture extends upward along the caving angle of the roof, and the development height of the fracture increases with it, as shown in Figures 12(b) and 12(c).

(3) Fractures stabilization stage: When the advance of the longwall face reaches critical mining, the development height of the upward fractures basically reaches the maximum value. Therefore, the longwall face continues to advance, and the upward fractures on the open cut side no longer developed, while the fractures on the longwall face side represent periodic development process of "fractures generation—fractures development and propagation—fractures stabilization—fractures closure-new fractures generation," but its development height is basically invariable, as shown in Figure 12(d).

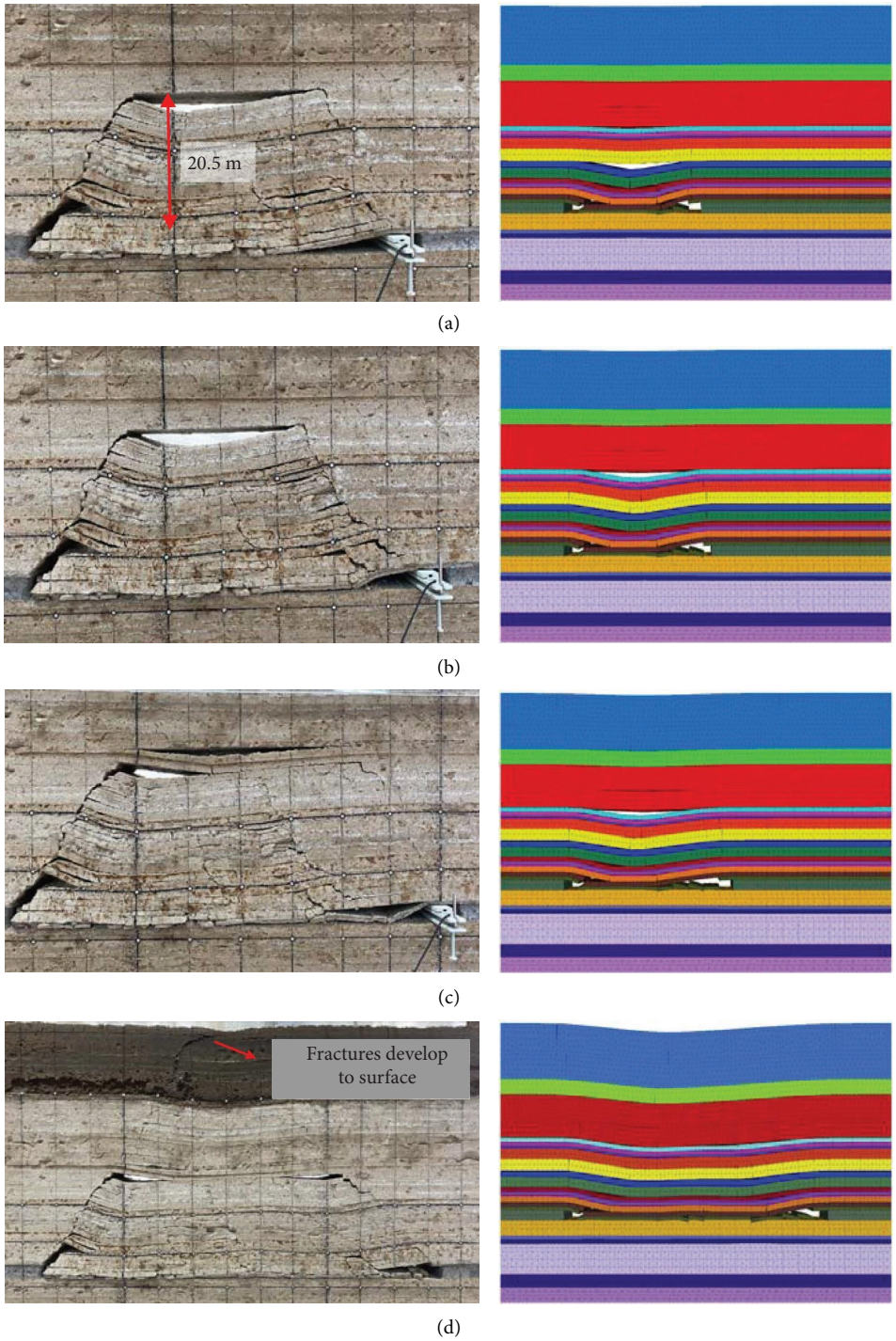

Figure 4: Periodic roof caving as face advances: (a) face advances to 54 m; (b) face advances to 64 m; (c) face advances to 76 m; (d) face advances to 120 m.

3. Development Mechanism of Upward Fractures Based on Fracture Growth Theory

3.1. Stress Analysis of Fracture End. The development of upward fractures is the result of the vertical force (weight of overlying strata) and concentrated tensile stress induced by roof caving. When the comprehensive stress reaches the ultimate tensile strength of rock, the rock strata will be damaged and generate fracture. Fracture mechanics can correlate the fracture strength of rock with the stress and is an effective method to analyze the development mechanism of upward fractures; therefore, fracture mechanics were used to analyze the stress and growth process of the fracture (Figure 13).

When the gravity G of the rock layer and the overburden load q act on the vertical direction of the fracture end, it can

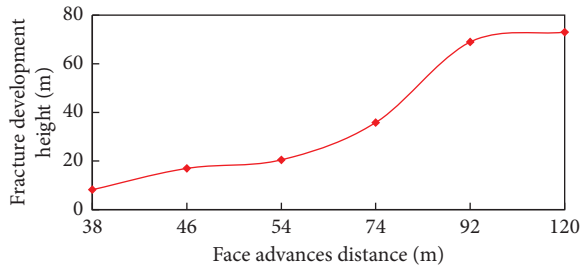

Figure 5: Fracture development height vs. longwall face advances.

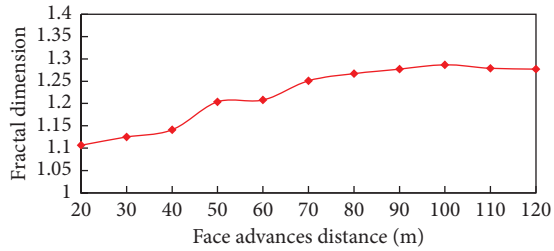

Figure 6: The fractal dimensions of fractures with different advance distances.

Figure 7: Physical simulation experiment model of Hongliulin Coal Mine.

Table 2: The material ratio of physical simulation experiment.

Lithology	Thickness (m)	Depth (m)	Consumables (kg)			
			Sand	Plaster	Calcium carbonate	Fly ash
Loess	39.00	39.00	Sand (56.16) : loess (16.16) : silicone oil (12.48)			
Red soil	30.80	69.80	Sand (56.16) : loess (16.16) : silicone oil (12.48)			
Siltstone	4.00	73.80	11.52	0.38	0.90	
Fine-grained sandstone	2.40	76.20	6.83	0.26	0.60	
Sandy mudstone	0.80	77.00	2.30	0.03	0.23	
Fine-grained sandstone	2.50	79.50	7.11	0.27	0.62	
Siltstone	10.60	90.10	30.53	1.02	2.37	
Fine-grained sandstone	3.00	93.10	8.53	0.32	0.75	
Medium-grained sandstone	2.10	95.20	5.97	0.15	0.60	
Fine-grained sandstone	1.50	96.70	4.32	0.14	0.34	
Medium-grained sandstone	7.40	102.60	21.05	0.52	2.11	
Fine-grained sandstone	3.30	105.90	9.39	0.35	0.82	
Coarse-grained sandstone	8.60	111.20	24.46	0.61	2.45	
Medium-grained sandstone	3.20	114.40	9.10	0.23	0.91	
Siltstone	2.40	113.60	6.91	0.23	0.54	
No. 4-2 coal seam	2.05	115.65	2.31	2.31	0.12	0.58
Medium-grained sandstone	1.40	117.05	3.98	0.10	0.40	

Figure 8: The immediate roof caves.

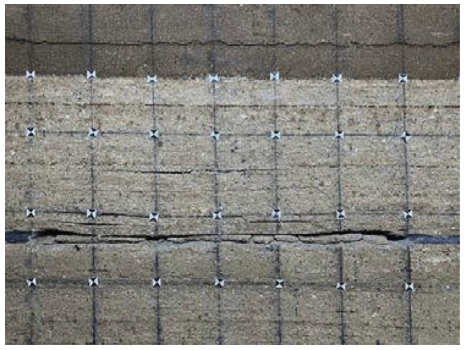

Figure 9: The first caving of main roof.

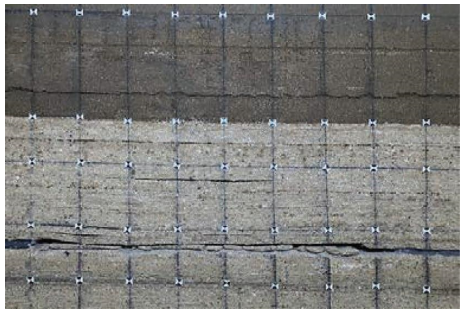

Figure 10: The roof caving with advances to 70 m.

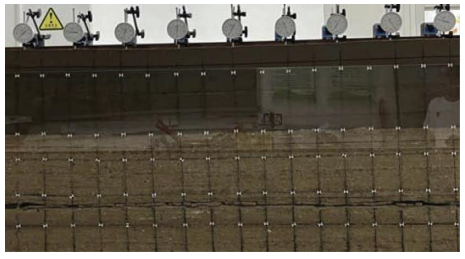

Figure 11: The roof caving with critical mining.

lead to in-plane shear fractures (Fracture type I in Figure 14(a)). When the boundary concentrated tensile stress σ_θ acts on the direction which is perpendicular to the upward fracture propagation direction, it can lead to tensile fractures (Fracture type II in Figure 14(b)).

The propagation of mining-induced fractures is the combined action of the previous two types of fractures. Therefore, it should be analyzed as mixed-type fractures (Fracture type I and II) in fracture mechanics, as shown in Figure 15.

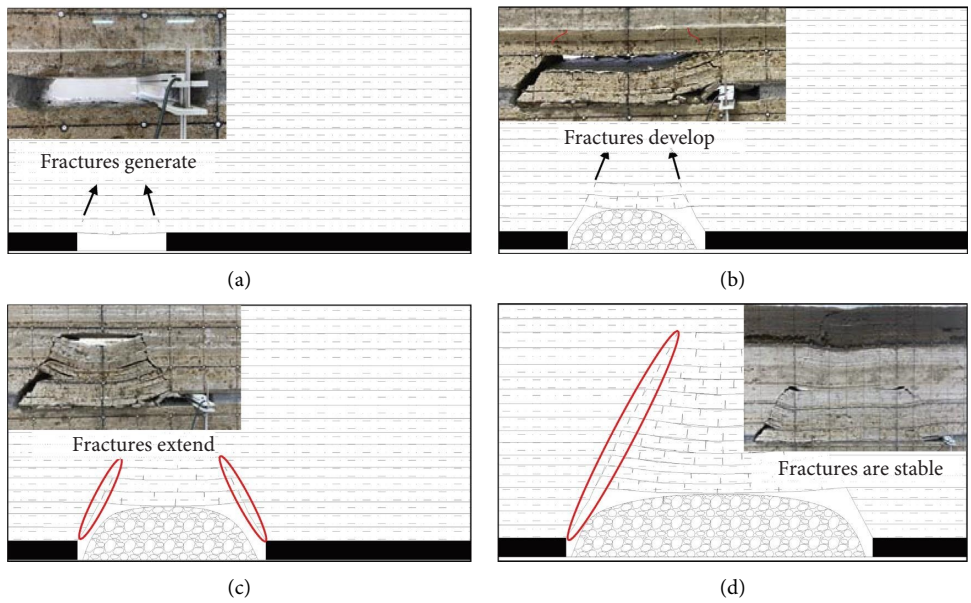

Figure 12: Development stage of mining-induced upward fractures: (a) fractures generate; (b) fractures develop; (c) fractures extend; (d) fractures stabilization.

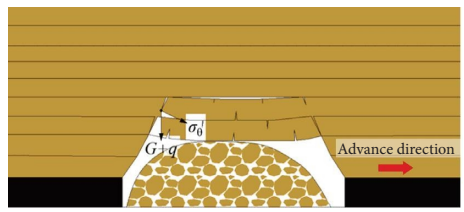

Figure 13: Stress analysis of fracture end.

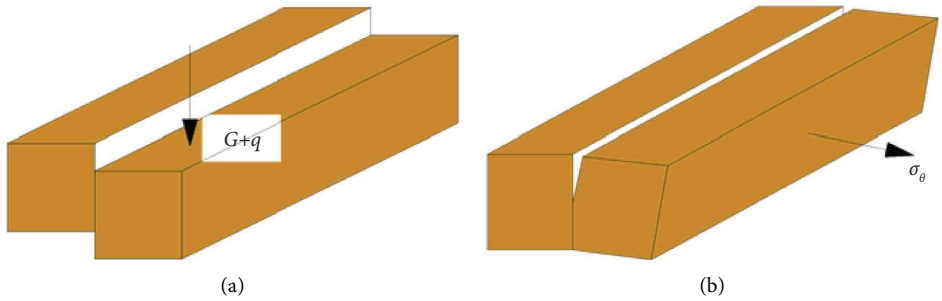

Figure 14: Two different fractures types: (a) in-plane shear fractures (fracture type I); (b) tensile fractures (fracture type II).

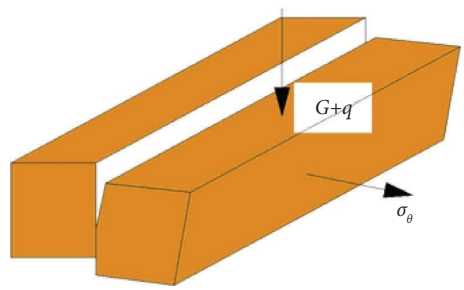

Figure 15: Mining-induced mixed-type fracture.

3.2. Development Mechanism of Upward Fractures. It is known that after longwall face mining, there are three zones along the vertical section of the rock strata. In caving zone, the caving roof represents disorder caving state, fractured zone is above caving zone, its roof shows as orderly caving, and broken roof shows that the upper part is stretched and the lower part is squeezed. In continuous deformation zone, there are no fractures that exist.

Due to the fact that the roof represents layered caving with mining, in order to analyze the development mechanism of the upward fracture in the fractured zone and determine its development height, the strata in the fractured zone were numbered from bottom to top (1, 2, ..., n), as shown in Figure 16.

The broken propagation of strata in fractured zone is calculated layer by layer from bottom to top. When the tensile stress and the vertical stress exceed its critical strength, fracture is first generated at the top of the rock layer, and then, under the effect of combined stress, the fracture will extend downward. If it penetrates through the rock layer, it will be broken and become a channel for water or gas conduction, and at the same time, the upward fracture develops and extends upward.

3.3. Determination Method for the Development Height of Upward Fractures. According to the development mechanism of upward fractures, with the increase of the calculated layer in fractured zone, when the fracture of No. $n-1$ layer can penetrate through the layer's free surface, this rock layer is completely broken, and the upward fracture can develop upwards. When the No. n layer is calculated, if the resultant stress is not large enough and cannot result in fracture propagation, the No. n layer is not broken completely; therefore, the upward fractures cannot develop upwards.

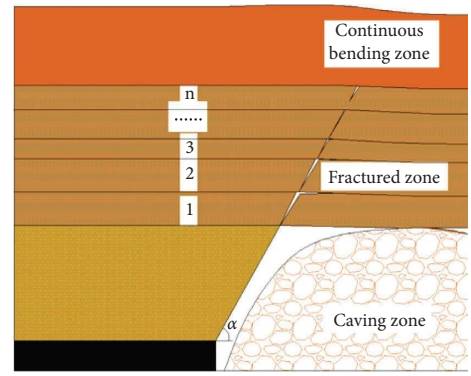

Figure 16: Development mechanism of upward fractures.

Based on the critical mining conditions, the method for the development height of upward fractures can be determined. Its development height is from the top of the coal seam to the bottom of the No. n rock layer, as shown in Figure 17.

4. Theoretical Model and Criterion of Fracture Propagation

4.1. $\sigma_{(\theta)max}$ Theoretical Model of Fracture Propagation. According to the $\sigma_{(\theta)\max}$ theory proposed by Li et al. [29], the parameter controlling the fracture of the rock stratum is the maximum hoop tensile stress $\sigma_{(\theta)\max}$ at the fracture end. Based on this, the theoretical model of fracture propagation is established (Figure 18).

The stress state at the fracture end is given as

$$\begin{cases} \sigma_r = \dfrac{1}{(2\pi r)^{(1/2)}}\cos\dfrac{\theta}{2}\left[K_I\left(1+\sin^2\dfrac{\theta}{2}\right)+\dfrac{3}{2}K_{II}\sin\theta-2K_{II}\tan\dfrac{\theta}{2}\right]+\cdots \\ \sigma_\theta = \dfrac{1}{(2\pi r)^{(1/2)}}\cos\dfrac{\theta}{2}\left[K_I\cos\theta-\dfrac{3}{2}K_{II}\sin\theta\right]+\cdots \\ \tau_{r\theta} = \dfrac{1}{(2\pi r)^{(1/2)}}\cos\dfrac{\theta}{2}\left[K_I\sin\theta+K_{II}(3\cos\theta-1)\right]+\cdots \end{cases}, \quad (2)$$

where θ is the fracture propagation angle, °. r is the distance from infinitesimal to fracture end, m. K_I is the strength factor of fracture type I, MPa · $\sqrt{\text{m}}$. K_{II} is the strength factor of fracture type II, MPa · $\sqrt{\text{m}}$. K_I and K_{II} can be calculated by the equations (3) and (4).

$$K_I = \sigma_\theta\sqrt{\pi c}, \quad (3)$$

$$K_{II} = \tau\sqrt{\pi c}, \quad (4)$$

where σ_θ is the tensile stress at point A, MPa. τ is the shear stress at point A, MPa. c is the half-length of the fracture, m, take $c = 1$, $r/c \ll 1$.

4.2. Establishment of Fracture Propagation Criterion. The fracture extends in the radial direction at its end. When $\sigma_{(\theta)\max}$ reaches the critical strength factor of the rock formation, the fracture starts to extends. According to

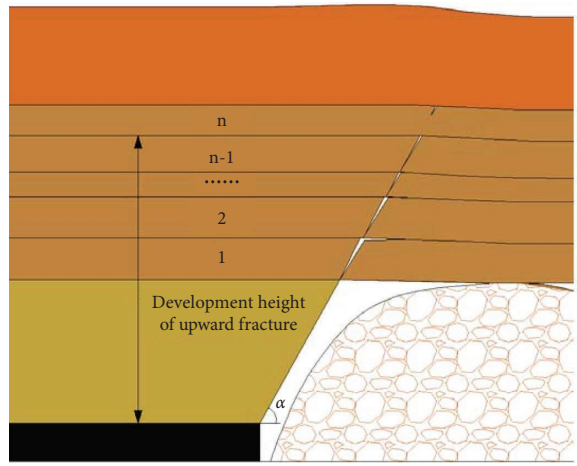

Figure 17: Determination of development height of upward fracture.

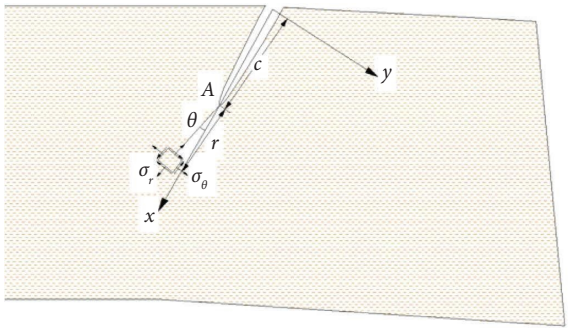

Figure 18: Theoretical model of fracture propagation.

equation (2), it can be expressed as equations (5) and (6) mathematically:

$$\cos\frac{\theta_0}{2}\left(\frac{K_I}{K_{Ic}}\cos^2\frac{\theta_0}{2}-\frac{3}{2}\frac{K_{II}}{K_{Ic}}\sin\theta_0\right)=1, \tag{5}$$

$$\cos\frac{\theta_0}{2}\left[K_I\sin\theta_0+K_{II}\left(3\cos\theta_0-1\right)\right]=0, \tag{6}$$

where K_{Ic} is the critical stress strength factor of fracture type I (material constant), MPa $\cdot\sqrt{\text{m}}$. K_{IIc} is the critical stress strength factor of fracture type II (material constant), and MPa $\cdot\sqrt{\text{m}}$. θ_0 is the fracture propagation initiation angle, °. According to equations (5) and (6), the fracture initiation trace of the $\sigma_{(\theta)\max}$ theory is obtained as shown in Figure 19.

The criterion for fracture propagation is as follows:

(1) According to equations (3), (4), and (6), the fracture propagation initiation angle θ_0 can be obtained.

(2) According to equations (3)–(5) and the value θ_0 calculated above, combining with Figure 19, it can be judged whether the fracture extends (whether the upward fractures develop).

If the coordinate (K_I/K_{Ic},K_{II}/K_{IIc}) is inside the fracture initiation trace, the fractures do not extend, and the mining-induced upward fractures do not develop upwards. On the contrary, if it is outside the fracture

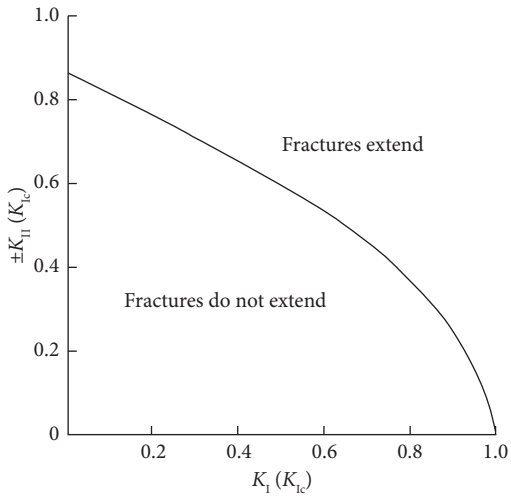

Figure 19: Fracture initiation trace of the $\sigma_{(\theta)\max}$ theory.

initiation trace, the fracture extends until it reaches the free surface, and the upward fracture continues to develop upwards.

5. Conclusions

The development of upward fractures can be divided into the following three stages: with the face advances from the open cut, the vertical fractures are generated at the mining boundary, and the roof is flexural but not caved; it is "Fractures generate stage." After roof caves, the upward fractures extend and develop upward along the caving angle with continue advances; it is "Fractures develop and extend stage." When the face reaches critical mining, the development height of the upward fractures is at its maximum and is basically invariable; it is "Fractures stabilization stage."

Mining-induced fractures can be analyzed as mixed-type fractures (in-plane shear fractures and tensile fractures) in fracture mechanics; when the combined stress exceeds the critical strength of stratum, it will extend downward until

penetrate through the stratum, and the upward fracture develops and extends upwards.

The parameter controlling the fracture of the rock stratum is the maximum hoop tensile stress $\sigma_{(\theta)\max}$ at the fracture end, the theoretical model of fracture propagation was established, and the criterion of upward fractures was proposed. If the coordinate $(K_I/K_{Ic}, K_{II}/K_{IIc})$ is inside the fracture initiation trace, the upward fractures do not develop upwards; on the contrary, the upward fracture continues to develop upwards.

Data Availability

The experimental data are all included within the article.

Conflicts of Interest

The authors declare that they have no conflicts of interest.

Acknowledgments

The authors thank the Natural Science Foundation of Inner Mongolia of China (grant number no. 2022QN05007) for its support in this study. This research was funded by the Natural Science Foundation of Inner Mongolia of China, grant number no. 2022QN05007, and Introduce Excellent Talents Support Project of Inner Mongolia, grant number no. 0701012101.

References

[1] W. Zhu and Y. H. Teng, "Characteristic of development of the fractured zone in mining under medium hard overburden using fully-mechanized top-coal caving method," *Applied Mechanics and Materials*, vol. 226, pp. 1312–1317, 2012.

[2] C. L. Zhang and Y. Zhang, "Stress and fracture evolution based on abutment change in thick coal seam—a case study in China colliery," *Electronic Journal of Geotechnical Engineering*, vol. 21, no. 12, pp. 4369–4386, 2016.

[3] Q. Bai and S. Tu, "A general review on longwall mining-induced fractures in near-face regions," *Geofluids*, vol. 2019, pp. 1–22, Article ID 3089292, 2019.

[4] Y. Tan, H. Cheng, W. Y. Lv et al., "Calculation of the height of the water-conducting fracture zone based on the analysis of critical fracturing of overlying strata," *Sustainability*, vol. 14, no. 9, p. 5221, 2022.

[5] H. F. Huang, Z. G. Yan, B. H. Yao, and H. J. Xu, "Research on the process of fracture development in overlying rocks under coal seams group mining in Wanli Mining Area," *Journal of Mining & Safety Engineering*, vol. 29, no. 5, pp. 619–624, 2012.

[6] Z. J. Wen, S. L. Jing, Y. J. Jiang et al., "Study of the fracture law of overlying strata under water based on the flow-stress-damage model," *Geofluids*, vol. 2019, Article ID 3161852, 12 pages, 2019.

[7] Z. L. Li, L. G. Wang, K. Ding et al., "Study on fracture and seepage evolution law of stope covered by thin bedrock under mining influence," *Minerals*, vol. 12, no. 3, p. 375, 2022.

[8] E. H. Bai, W. B. Guo, Y. Tan et al., "Regional division and its criteria of mining fractures based on overburden critical failure," *Sustainability*, vol. 14, no. 9, p. 5161, 2022.

[9] J. L. Xu, X. Z. Wang, W. T. Liu, and Z. G. Wang, "The influence of the location of the main key strata on the height of the water flowing fractured zone," *Journal of Rock Mechanics and Engineering*, vol. 28, no. 02, pp. 380–385, 2009.

[10] J. L. Xu, W. B. Zhu, and X. Z. Wang, "Height prediction method of water flowing fractured zone based on key stratum position," *Coal Journal*, vol. 37, no. 05, pp. 762–769, 2012.

[11] W. Z. Zhang and Q. X. Huang, "Study on the development height of upward fissures in local filling mining of shallow coal seams," *Coal Mine safety*, vol. 45, no. 04, pp. 40–42, 2014.

[12] B. C. Zhao, H. Sun, Y. X. Guo, and X. Yang, "Research on dynamic evolution law of water-conducting fracture in thick loose layer near shallow coal seam mining," *Coal Engineering*, vol. 53, no. 10, pp. 100–105, 2021.

[13] J. Cao and Q. X. Huang, "Regularity and control of overburden and surface fractures in shallow-contiguous seams," *Coal Geology & Exploration*, vol. 49, no. 4, pp. 213–220, 2021.

[14] T. Liang, X. L. Liu, and S. J. Wang, "Fractal study on the crack network evolution and permeability change in mining rock mass," *Journal of China Coal Society*, vol. 44, no. 12, pp. 3729–3739, 2019.

[15] L. H. Guo, H. Cheng, S. L. Peng, and B. J. Fu, "Study on evolution and subsidence fractal characteristics of overlying strata in thick loose layers and thin bedrocks," *Safety In Coal Mines*, vol. 51, no. 9, pp. 59–64, 2020.

[16] D. P. Li, H. W. Zhou, D. J. Xue, H. Y. Yi, and H. L. Gao, "Relationship between percolation and fractal properties of mining-induced crack network in coal and rock masses," *Rock and Soil Mechanics*, vol. 36, no. 4, pp. 1135–1140, 2015.

[17] S. G. Li, W. B. Qin, Z. L. Li, Y. Ding, and H. F. Lin, "Research on fractal characterization of mined crack network evolution repeated coal mining," *Journal of Liaoning Technical University*, vol. 35, no. 12, pp. 1384–1389, 2016.

[18] X. S. Li, Q. H. Li, Y. J. Hu et al., "Study on Three-dimensional dynamic stability of open-pit high slope under blasting vibration," *Lithosphere*, vol. 2021, no. 4, Article ID 6426650, 2022.

[19] D. Z. Ren, X. Z. Wang, Z. H. Kou et al., "Feasibility evaluation of CO2 EOR and storage in tight oil reservoirs: a demonstration project in the Ordos Basin," *Fuel*, vol. 331, Article ID 125652, 2023.

[20] M. C. He, Q. R. Sui, M. N. Li, Z. J. Wang, and Z. G. Tao, "Compensation excavation method control for large deformation disaster of mountain soft rock tunnel," *International Journal of Mining Science and Technology*, vol. 32, no. 5, pp. 951–963, 2022.

[21] C. Zhu, M. C. He, B. Jiang, X. Z. Qin, Q. Yin, and Y. Zhou, "Numerical investigation on the fatigue failure characteristics of water-bearing sandstone under cyclic loading," *Journal of Mountain Science*, vol. 18, no. 12, pp. 3348–3365, 2021.

[22] Q. Wang, S. Xu, Z. X. Xin, M. C. He, H. Y. Wei, and B. Jiang, "Mechanical properties and field application of constant resistance energy-absorbing anchor cable," *Tunnelling and Underground Space Technology*, vol. 125, Article ID 104526, 2022.

[23] C. Zhu, X. D. Xu, X. T. Wang et al., "Experimental investigation on nonlinear flow anisotropy behavior in fracture media," *Geofluids*, vol. 2019, no. 9, Article ID 5874849, 9 pages, 2019.

[24] Y. D. Bao, J. P. Chen, L. J. Su, W. Zhang, and J. W. Zhan, "A novel numerical approach for rock slide blocking river based on the CEFDEM model: a case study from the Samaoding paleolandslide blocking river event," *Engineering Geology*, vol. 312, Article ID 106949, 2023.

[25] Q. Wang, B. Jiang, S. Xu et al., "Roof-cutting and energy-absorbing method for dynamic disaster control in deep coal

mine," *International Journal of Rock Mechanics and Mining Sciences*, vol. 158, Article ID 105186, 2022.

[26] S. B. Tang, J. M. Li, S. Ding, and L. T. Zhang, "The influence of water-stress loading sequences on the creep behavior of granite," *Bulletin of Engineering Geology and the Environment*, vol. 81, no. 11, p. 482, 2022.

[27] X. Liang, S. B. Tang, C. A. Tang, L. H. Hu, and F. Chen, "Influence of Water on the Mechanical Properties and Failure Behaviors of sandstone under Triaxial Compression," *Rock Mechanics and Rock Engineering*, pp. 1–32, 2022.

[28] Y. Wang, C. Zhu, M. C. He, X. Wang, and H. L. Le, "Macro-meso dynamic fracture behaviors of Xinjiang marble exposed to freeze thaw and frequent impact disturbance loads: a lab-scale testing," *Geomechanics and Geophysics for Geo-Energy and Geo-Resources*, vol. 8, no. 5, 154 pages, 2022.

[29] H. Li, Z. G. Yin, J. Xu, and W. W. Zhang, *Rock Fracture Mechanics*, Chongqing University Press, Chongqing, China, 1988.